New Results on Bistability Effects in HEB Devices

Dazhen Gu, Yan Zhuang, Sigfrid Yngvesson
Department of Electrical and Computer Engineering, University of Massachusetts, Amherst, MA 01003

The Hot Electron Bolometric (HEB) mixer, employing NbN superconducting material, has been widely used as the terahertz (THz) receiver [1][2][3]. The essential part of the HEB device is a thin NbN film which is a fraction of a μm long and a few μm wide. Several models have been developed to predict its performance in the THz frequency range. The hot spot model, based on nonlinear heat transfer and self-heating, is the most popular theory and is the one that best fits the experimental results.

The operating condition for an HEB device is normally at liquid Helium temperature, which allows the NbN material to work as a superconductor. At some specific DC bias conditions, a hot spot is sustained by *Joule* heating, which is sufficient to raise the temperature above T_C, i.e. the critical temperature of superconductor. The rest of the NbN micro strip is still superconducting. This phenomenon can be explained by the heat balance equation holding at more than one temperature. Due to an external perturbation, the hot spot can recover to the superconducting state or vice versa. The device is thus *bistable* state. To understand the details of this mechanism will improve the hot spot model, since the optimal HEB device operating point for the mixer is just in this region.

1. Steady Hot Spot in a Superconduting Strip

The non-uniform thermal structure in a superconducting strip could be described as a hot region (hot spot), where electrons become normal, and a cold region, where they maintain their superconductivity. The heat balance equations for this strip can be represented as:

$$-\frac{\partial}{\partial x}\left(K_N \cdot \frac{\partial T}{\partial x}\right) + q = Q \qquad x<x<x_0, \text{ (normal region)} \quad \text{(1a)},$$

$$-\frac{\partial}{\partial x}\left(K_S \cdot \frac{\partial T}{\partial x}\right) + q = 0 \qquad x_0<x<L/2, \text{ (superconducting region)} \quad \text{(1b)}.$$

Here, we assume a device of length L, width W, and thickness d with a normal region of length $2x_0$ and resistivity ρ_N. Q is the power of the *Joule* heating, q is the specific power due to heat transfer to a cold bath. K_N and K_S are the thermal conductivity in the normal region and superconducting regions respectively, which are assumed identical, equal to K and estimated from the resistivity by the *Wiedemann-Franz Law*:

$$K \cdot \rho_N = \frac{\pi^2}{3}\left(\frac{k_B}{e}\right)^2 \cdot T \qquad (2).$$

Solving Equation (1), we'll have an analytical solution for the non-uniform temperature distribution. A more rigorous approach has been applied by H. Merkel [4], who included the Andreev Reflection and localized device parameters in Equation (1).

2. A Dynamic Hot Spot in Superconducting Strip

Starting with the time-independent heat balance Equations (1a) and 1 (b), we can rewrite these including a time-dependence: $$C\frac{\partial T}{\partial t}=\frac{\partial}{\partial x}\left(K\frac{\partial T}{\partial x}\right)+Q-q \quad (3),$$

where C is the heat capacity of the superconductor per unit volume. In a general case, the temperature-dependent Q and q are plotted in Figure 1. Self-heating in a superconductor has three parts: (1) when the temperature is lower than the effective critical temperature T_{Ceff} (obtained from the *Ginsburg-Landau* relation), there is no heating power, $Q=0$; (2) when the temperature is higher than T_C, the superconductor becomes totally normal, $Q=J^2\rho_N$. (3) when the temperature is in the range of (T_{Ceff}, T_C), $Q=J^2\rho_N(T-T_{Ceff})/(T_C-T_{Ceff})$. Here, J is the current density in the region of interest.

The uniform central temperature is determined by $Q=q$, since the values of $\partial T/\partial t$ and $\partial T/\partial z$ are both zero near the center. In other words, the current should be high enough to elevate curve Q to intersect with curve q, as shown in Figure 2. Of the two intersections (at T_1 and T_2), only T_2 is stable against small perturbations. Let's consider two cases for state 2: (1) if it is perturbed by a small increase in temperature, the cooling curve q will exceed the heating curve Q, and make the temperature fall back to T_2; (2) on the other hand, if it is perturbed by a small decrease in temperature, the heating curve Q will exceed the cooling curve q, and make temperature go up to T_2. As for state 1, a small increase in temperature will lead to temperature elevation to T_2 and a small decrease in temperature will cause the temperature to fall to T_b. Thus, for a stable normal zone, its central temperature must be at T_2.

Consider the domain wall (i.e. the transition region at the edge of the hotspot where the temperature goes from T_1 to T_2) propagating as: $z = x + v\cdot t$, substitute this into Equation (3), which yields:

$$-vC\frac{dT}{dz}+\frac{d}{dz}\left[K\left(\frac{dT}{dz}\right)\right]+Q-q=0 \quad (4).$$

To derive the minimum propagating current I_p, set $v=0$ in Equation (4), then follow the same algebraic steps as in Reference [5]. We obtain the well-known equal-areas theorem for I_p: $\int_{T_b}^{T_2}(Q-q)dT=0$ (5), i.e., the two hatched areas in Figure 3 should be equal under the condition of minimum domain propagation.

When the current lies beyond (or below) the minimum propagating current I_p, the hot spot grows (or shrinks) due to more (or less) self-heating than heat transfer. Under the constant current bias condition, the propagating velocity is constant and the temperature profile at the edges of the hot spot does not change its shape with time. To calculate this velocity, we employ equation (4), using the heat flux, which is defined as $s=K(dT/dx)$: $$-vCs+s\left(\frac{ds}{dT}\right)+K(Q-q)=0 \quad (6).$$

To avoid the complexity of solving this equation, we make the following approximations: (1) replacing the three-part curve for Q by a two-part step function curve: $g(\Delta T)=\rho_N\cdot J^2$ for $\Delta T<(T_C+T_{Ceff})/2-T_b$ and $g(\Delta T)=0$ for $\Delta T>(T_C+T_{Ceff})/2-T_b$; (2) using *Newton*'s law of cooling $q=h\cdot\Delta T/d=h\cdot(T-T_b)/d$, where we ignore

the nonlinear case; (3) assuming K is temperature independent. The approximate analytical solution of the velocity is given by: $$v = v_* \frac{C_0 - 1}{2\sqrt{\alpha}\sqrt{C_0}} \quad (7),$$

where, v_* is the characteristic thermal velocity: $v_* = \frac{2J_c}{C}\sqrt{\frac{K\rho_N}{\Delta T_c}}$; α is the so called *Stekly* number

$\alpha = \frac{\rho_N J_c^2 d}{h\Delta T_c}$, which characterize the relative role of *Joule* self-heating in the superconductor; C_0 is a function dependent of the current density as: $C_0 = \frac{\alpha i^2 - (1 - i/2)}{1 - i/2}$, with normalized current density: $i=J/J_C$.

The plots of the normalized velocity and the normalized current are shown in Figure 3.

3. Experimental Setup

The whole experimental setup for recording the device behavior is shown in Figure 4. The device is mounted on a circuit board in an Aluminum box. We bias the device through a low pass filter by a very low resistance voltage source. The box is immersed into Liquid Helium and is connected to two coaxial cables housed in a stainless steel tube.

With the aid of an oscilloscope, which has an upper limit of 1 GHz, we detect the voltage response from two SMA connectors on the box. One is the voltage across the reference resistor, which can be converted to the current through the device. The other is the total voltage across the device and the reference resistor.

Another experimental setup is employed for the domain velocity measurement. A pulse generator, paralell with the DC bias box, is added to drive the device from the superconduting state to the normal state, and vice versa. We also include a resistor with several hundred ohms between the bias box and device box . This resistor will enable us to measure the voltage and current waveform of the device more accurately.

4. Measurements on NbN Films

The devices used for instability measurements are NbN strips with several different lengths and widths, which are fabricated by standard UV lithography.

4.1 Self Sustained Oscillation

Figure 5(a) and 5(b) show the oscillations from a voltage-biased device with dimensions $1X2\mu m^2$ at different bias points. At this point, we removed the reference resistor from the Aluminum box to check the pure voltage response of the device.

In the beginning, at the lower bias voltages, the oscillation response is similar to that in Figure 5(a). Besides the fast 25 MHz relaxation oscillation, there is another slow oscillation modulating on it, which we will call the slow repetition frequency. It separates the whole response into two parts: (1) the upper level oscillation, which means that the device is mainly "hot" and exhibits a voltage value; (2) the lower level

oscillation, which means that the device is mainly "cold" and the average voltage is zero. When we increase the bias voltage, the repetition frequency also increases, in other words, the adjacent upper levels become closer. However, the 25 MHz relaxation oscillation doesn't change with the bias.

The repetition frequency was also observed in other work, for example in [6] and in [7,8]. It can be shown [6,8] that this frequency depends on the inductance in series with the device, as well as the bias voltage, in quantitative agreement with experiment.

The voltage response of device, biased at some ***high*** voltage point, is shown in Figure 5(b), where the lower level oscillation disappears. We interpret the variation of the device voltage as being due to the (normal) hotspot varying periodically in size. The thermal domain (hot spot) in the device will propagate from infinitesimal to some finite length. Further increase of the bias voltage will only increase the amplitude of the oscillation, which corresponds to the maximum length of the domain.

We then I added the 20Ω reference resistor to investigate both the voltage and current response, which are shown in Figure 6(a). Both voltage and current show the 25MHz relaxation oscillation. However, no matter where the bias is set, we can't find the simple sinusoidal relaxation oscillation from this measurement setup. Our interpretation of this is that the reference resistance stabilizes the device, as was also observed in [7,8]. By switching the 20Ω resistor to a 5Ω resistor, we obtain the pure oscillation again, shown for both current and voltage in Figure 6(b).

We repeated the measurements on several different devices both on silicon substrate and on MgO substrate. From the results listed in Table 1 the 25 MHz relaxation oscillation seems to be an intrinsic property of the NbN film, independent of the device dimension and the device wafer. This oscillation nevertheless seems sensitive to the exact experimental setup, since in earlier measurements in a slightly different experimental arrangement we measured this frequency as about 5 MHz [7,8].

4.2 Fly-out Measurements

In this section, we describe a measurement to investigate the hot spot domain expansion, which we call "fly-out". The experimental setup is shown in Figure 4. There is a resistor of several hundred ohms in series with the device. The device has a second stable state at higher voltage and lower current, shown in Figure 7.

We bias the device is at 745μA, which is close to its critical current, and then apply a positive pulse to drive the device to its normal state, which will stimulate a hot spot domain in the device. The positive pulse has a small amplitude and short duration, which won't have any effect on the device after this short time. After the domain wall has expanded to its equilibrium state, a negative pulse makes the device go back to its superconducting state. With the aid of the oscilloscope, we record both the device voltage and reference voltage, which can be converted to the device current. Figure 8 shows the voltage and current waveforms. The device shifts repeatedly between superconducting and normal state under double pulses.

To prove that the response shown in Figure 8 is an intrinsic device property, we also measured the voltage waveform on a dummy resistor under the same pulse, shown in Figure 9. Comparing the responses

of the device and the resistor, we can confidently claim that the device responds to the pulse much more slowly, due to the hot spot domain wall propagation.

During the domain wall expansion, we assume that the hot spot resistivity is constant, which is equal to the resistivity of device in the low temperature normal state: $\rho = R_N \frac{A}{L}$ (8),

where A and L are device cross section area and length respectively, and R_N is the full device normal resistance at low temperature. Then the device resistance is proportional to its hot spot length. Thus the velocity of the domain expansion can be obtained by:

$$v = \frac{1}{2}\frac{dl_{domain}}{dt} = \frac{1}{2}\frac{d(R \cdot A/\rho_N)}{dt} = \frac{1}{2}\frac{L}{R_N}\frac{dV}{dt}\frac{1}{I} \quad (9).$$

Here, the factor 2 represents the fact that two domain walls are involved in the propagation. As the domain expands, the current shows small oscillations around a constant value. By varying this average current we can plot v as a function of I, or normalized v versus normalized I.

4.3 Fly-back Measurements

Besides fly-out measurements, we designed another measurement setup for testing the domain as its size was shrinking. Now we applied a DC bias to the device to set its current slightly smaller than the domain wall minimum propagation current I_p. Two pulses were then applied. The first pulse was about 0.3μs long and had large amplitude to stimulate a hot spot in the device. The second pulse resulted in a total current value slightly larger than I_p and was applied to the device with much longer duration to let the device be stable in the normal state. Following the second pulse, the hot spot domain is predicted to shrink by itself. We could observe the voltage waveform decreasing linearly until it reached zero, while the current stayed at an intermediate value for a short duration. We believe that this intermediate current is equal to I_p. The waveforms are shown in Figure 10. Because of this constant current level, we can't follow the same method for calculating the domain velocity as we do in the case of the fly-out.

From the recording of the voltage waveform, we can obtain the relaxation time τ of the domain wall shrinking under different DC bias. This relaxation time is found to be independent of the amplitude and width of the second pulse. However, it is dependent on the DC bias current. This agrees with the measurements by *Freytag* and *Huebener* [9], who made similar measurements on Sn film We assume that the current in the device is equal to the DC bias current after the second pulse. Thus we can approximately calculate the fly-back velocity as: $v(I_{DC}) = \frac{L}{\tau}$.

5. Discussion of Experimental Results

In order to fit the experimental velocity with the theoretical *v-i* curve (Figure 3), we need to obtain the characteristic thermal velocity v_* and the *Stekly* number α for this particular device. The calculated thermal velocity for this device is v_*=107m/s, and the *Stekly* number is α=36. By fitting the fly-out velocity shown in Figure 8, we find that the *Stekly* number is 13 for the best least square fit. This discrepancy may come from the measurements on critical current and the estimation of film thickness.

The experimental data agree well with the prediction based on Eq. (7) if we multiply the experimental resuls by a factor of 10, and normalize them to v_{*}. This big discrepancy may come from the thermal conductivity K of NbN film even after including the *Andreev* Reflection effect. This value is strongly related to the film thickness, substrate type and cryogenic condition. A more likely explanation is that the theory in [5] assumes a quasi-steady state in which the domain propagates at a constant velocity. The actual conditions are likely a good deal more nonlinear, which could slow the propagation of the domain [9].

On the other hand, we get some reasonable results from Figure 11. First, the minimum propagation current can be calculated from the plot by interpolating the curve: $0.347*I_C \approx 300\mu A$. This is very close to the result of the fly-back measurements, i.e., the constant current level in Figure 10. Secondly, the fly-back velocity grows much faster than the fly-out velocity, as the current deviates from I_p, based on the experimental results, which agrees with the theory very well. Third, the value of the *AR* factor α_{th} (from the best fitting curve) is very close to the theoretical value at 4K from theoretical value. Finally, if we calculate the relaxation oscillation frequency from the same domain velocity model, we obtain order-of-magnitude agreement; this oscillation is also *slower,* but by a factor of about 6 compared with the model. As a conclusion, the domain wall propagation model predicts the trend of the velocity curve very well, and the order-of-magnitude of the relaxation frequency. The maximum amplitude of the oscillation is also always less or equal to that obtained from a domain which fully fills the device length. To improve the agreement between theory and experiment, we have to put more emphasis on estimating accurate parameters for the device, such as thermal conductivity, heat transfer coefficient and device dimension. We also need to explore a more realistic nonlinear model for the domain dynamics.

Reference:

[1] E. Gerecht et al, Proc. 14th Intl. Symp. Space Terahertz Technology, Tucson, USA, April 2003.

[2] S. Cherednichenko, et al, Proc. of the Symp. on Astronomical Telescopes and Instrumentation, SPIE, Hawaii, USA, August 2002.

[3] D. J. Benford et al, Proc. 14th Intl. Symp. Space Terahertz Technology, Tucson, AZ, April 2003.

[4] H. Merkel, Proc. 13th Intl. Symp. Space Terahertz Technology, Cambridge, USA, April 2002.

[5] L. Dresner, "Stability of Superconductors", Plenum Press, NY, 1995.

[6] V. N. Skokov, Technical Physics Journal, 40, 562-565, 1995.

[7] Y. Zhuang et al, Proc. 14th Intern. Symp. Space THz Technology, Tucson, AZ, Apr. 2003.

[8] Y. Zhuang, PhD Thesis, UMass Amherst, 2002.

[9] L. Freytag and R. P. Huebener, J. Low Temp. Phys. 60 (1985) 377.

[10] H. Merkel, private communication.

Table 1: Relaxation oscillation frequency for different devices.

Substrate	Silicon						MgO	
Dimension (μm^2)	1X2	4X2	5X2	10X2	5X5	10X5	4X2	5X5
Frequency (MHz)	25.5	25.5	24.9	25.5	26.8	25.9	26.8	26.8

Figures

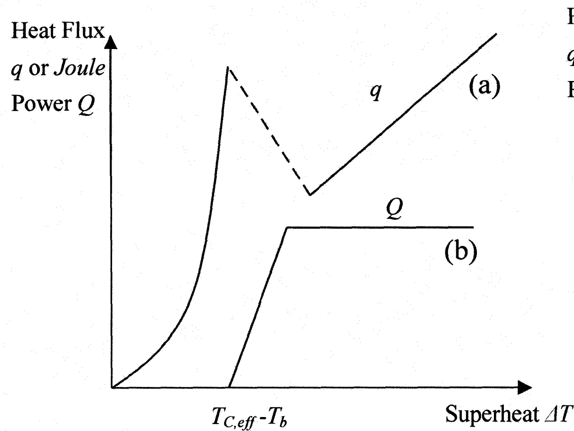

Figure 1: The steady state boiling heat flux with the three-part curve of *Joule* power.

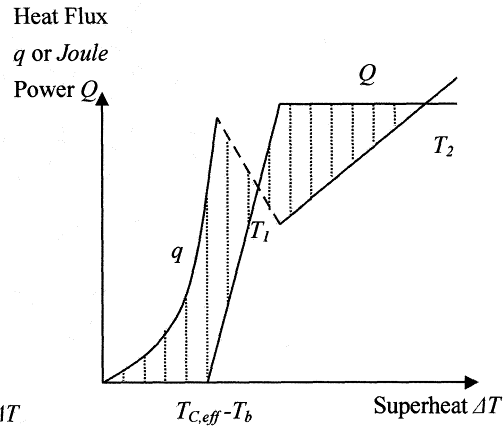

Figure 2: The steady state boiling heat flux intersects the three-part curve of *Joule* power. The equality of the two hatched region determines I_p.

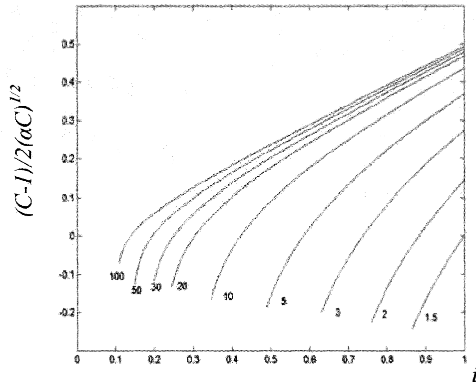

Figure 3: Normalized velocity versus normalized current under different *Stekley* number.

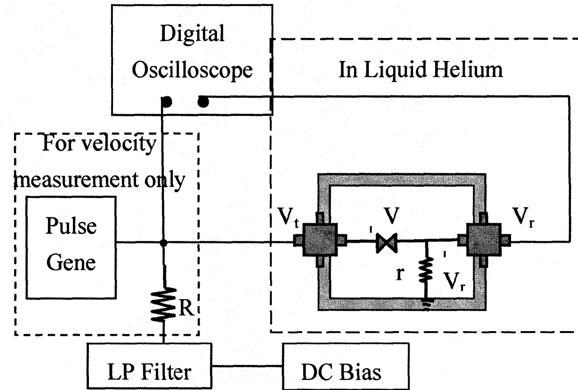

Figure 4: Experimental setup for the instability oscillation / (domain velocity) measurement.

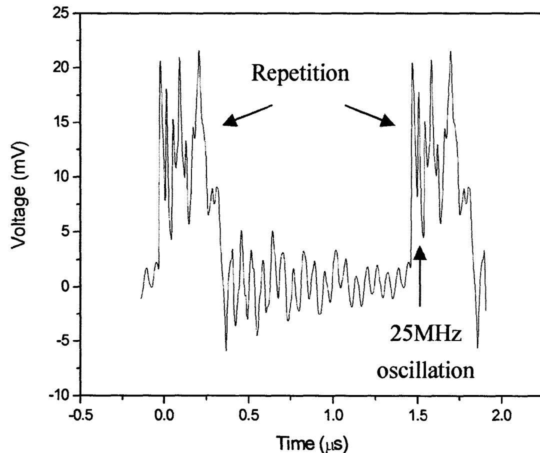

(a) Bias at 3.3 mV, 121μA.

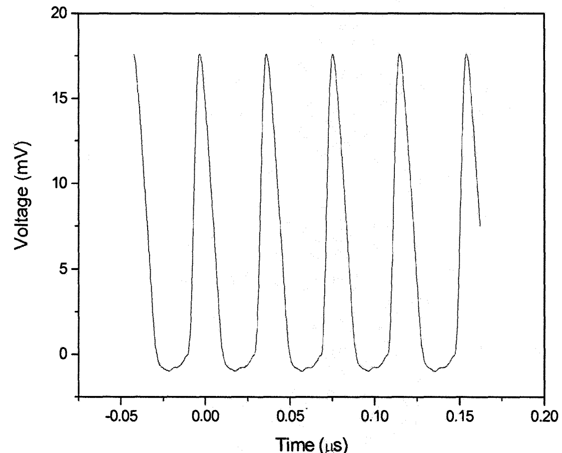

(b) Bias at 4.7 mV, 125μA.

Figure 5: Voltage waveform of one device (1X2μm^2) in unstable region without reference resistor.

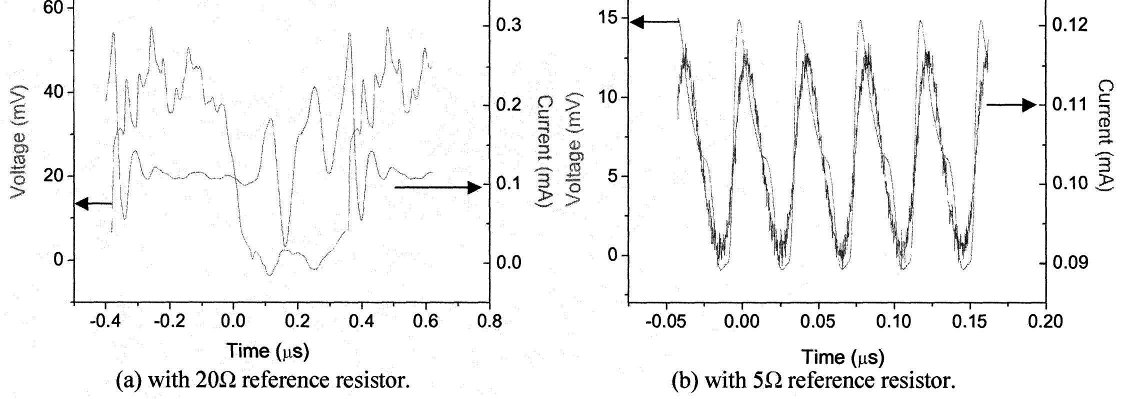

(a) with 20Ω reference resistor. (b) with 5Ω reference resistor.

Figure 6: Voltage and current waveforms of NbN device in unstable region with measurement setup in Figure 4.

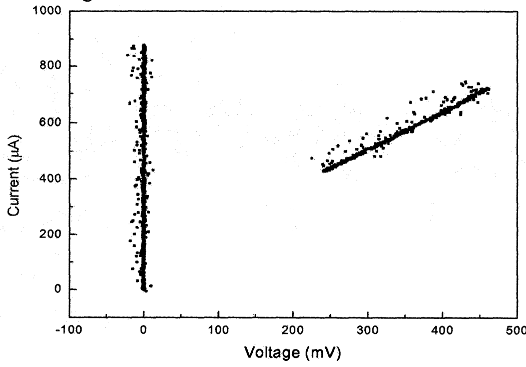

Figure 7: IV curve of the 5μm long device.

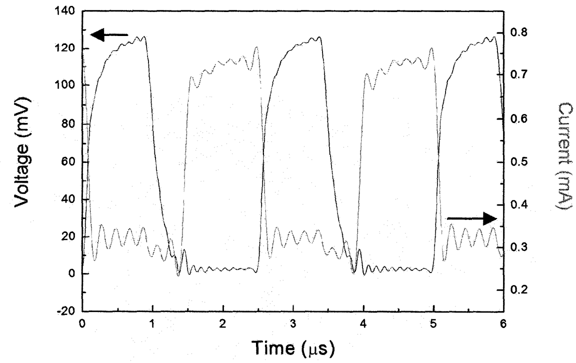

Figure 8: Voltage and Current response of device 5μm long device under double pulses.

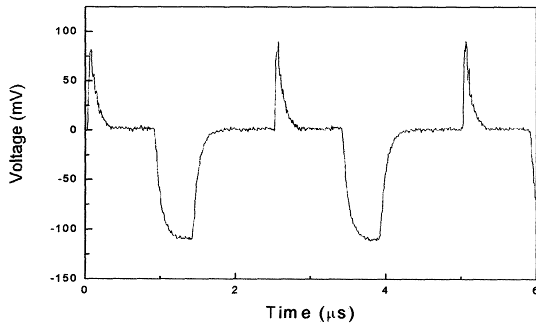

Figure 9: Voltage response of a dummy resistor under double pulses.

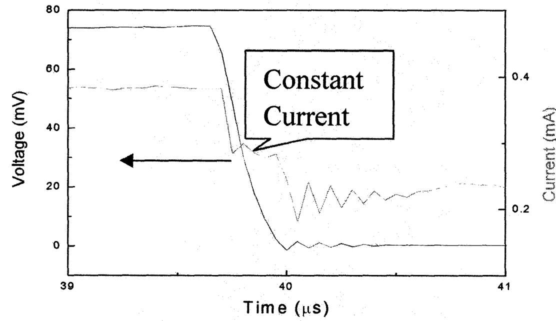

Figure 10: Voltage and current waveform in the fly back measurement 5μm long device.

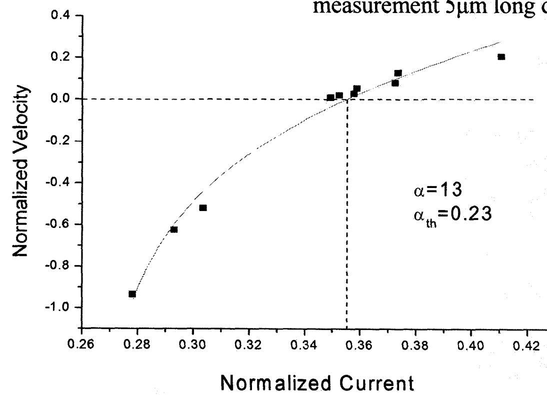

Figure 11:Comparison between the theory and the experimental results on fly-out and fly-back measurements for 5μm long device.